

We are IntechOpen, the world's leading publisher of Open Access books Built by scientists, for scientists

6,900

Open access books available

186,000

International authors and editors

200M

Downloads

Our authors are among the

154

Countries delivered to

TOP 1%

most cited scientists

12.2%

Contributors from top 500 universities



WEB OF SCIENCE™

Selection of our books indexed in the Book Citation Index
in Web of Science™ Core Collection (BKCI)

Interested in publishing with us?
Contact book.department@intechopen.com

Numbers displayed above are based on latest data collected.
For more information visit www.intechopen.com



Diffuse Dielectric Anomalies in CoTiO_3 at High Temperatures

C. C. Wang, M. N. Zhang, G. J. Wang, and K. B. Xu
*Laboratory of Dielectric Functional Materials, School of Physics and Material Science,
Anhui University, Hefei
P. R. China*

1. Introduction

The ABO_3 -type materials with ilmenite structure have been studied extensively as functional inorganic materials due to their weak magnetism and semiconductivity. They find wide applications such as pigment, gas sensor for ethanol, high performance catalysts, electrodes of solid oxide fuel cells, and microwave dielectric resonator, etc [1-7]. As a typical ilmenite structure material, Cobalt titanate, CoTiO_3 (CTO), has received considerable research interest in recent years due to its dielectric properties [8]. This material appears to be a promising high-k dielectric material in semiconductor devices like Metal-Oxide-Semiconductor Field-Effect Transistors and Dynamic Random Access Memories [9-11]. This promising prospect requires a full characterization of the dielectric properties of CTO in the case of both thin film and ceramics around room temperature. In our previous work [8], we reported the low-frequency ($10^2\sim 10^5$ Hz) dielectric properties of CTO ceramics in the temperature range between 130 and 430 K. Two dielectric relaxations were found with the low-temperature one ascribed to the dipolar effect induced by charge-carrier hopping motions and the high-temperature one related to the defect dipolar polarization created by Co vacancies and Ti^{3+} ions. This work revealed some interesting dielectric features of CTO at low temperatures. Nevertheless, the high-temperature dielectric properties of this material have not been reported so far. Hence, the aim of this work is to investigate, in details, the dielectric properties of CTO ceramics at high temperatures ranging from room temperature to 800 °C. Two diffuse dielectric anomalies were found and their physical natures were discussed.

2. Experimental details

Single phased CTO ceramic samples used for dielectric measurements were prepared by solid-state reaction using high purity (99.99%) starting powders of Co_3O_4 and TiO_2 . Details about the sintering processes were reported in our preceding paper [8]. The purity of the resultant compound was examined by powder X-ray diffraction (XRD) on a XD3 diffractometer. The structural properties of CTO at high temperatures were measured from room temperature to 900 °C using a MXP18AHF system with a high-temperature attachment and analyzed using Jade refinement. To modify the dielectric properties of CTO ceramics, excess Co_3O_4 powder was added into the resultant CTO powder. The mixture was

thoroughly ground, palletized, and sintered at 1050 °C for 20 h. Annealing treatments were performed in flowing (200 ml/min) O₂ and N₂ (both with purity >99.999%) at 800 °C for 2 h. The temperature-dependent dielectric properties were obtained using a Wayne Kerr 6500B precise impedance analyzer with the sample mounted in a holder placed inside a PST-2000HL dielectric measuring system. The temperature variations were automatically controlled using a Stanford temperature controller with a heating rate of 3 °C/min. The system can provide a high temperature range from room temperature to 1000 °C. The ac measuring signal was 100 mV rms. Electrodes were made by printing Pt paste on both sides of the disk-type samples and then fired at 800 °C for 1 h in order to remove the polymeric component.

3. Results and discussion

Figure 1 shows a representative diagram of the variation in dielectric constant (ϵ' , the real part of the complex permittivity) with temperature at various frequencies for an as-prepared CTO pellet (with diameter of ~ 12 mm and thickness of 1.82 mm). At first glance, $\epsilon'(T)$ exhibits two diffuse dielectric anomalies located at 250 °C and 600 °C, respectively. Both anomalies are characterized by: (i) a broad peak in $\epsilon'(T)$, with the peak getting smaller and shifting to higher temperature as the measuring frequency increases; and (ii) the low-temperature side of the peak shows strong frequency dispersion, whereas the high-temperature side almost exhibits frequency independence.

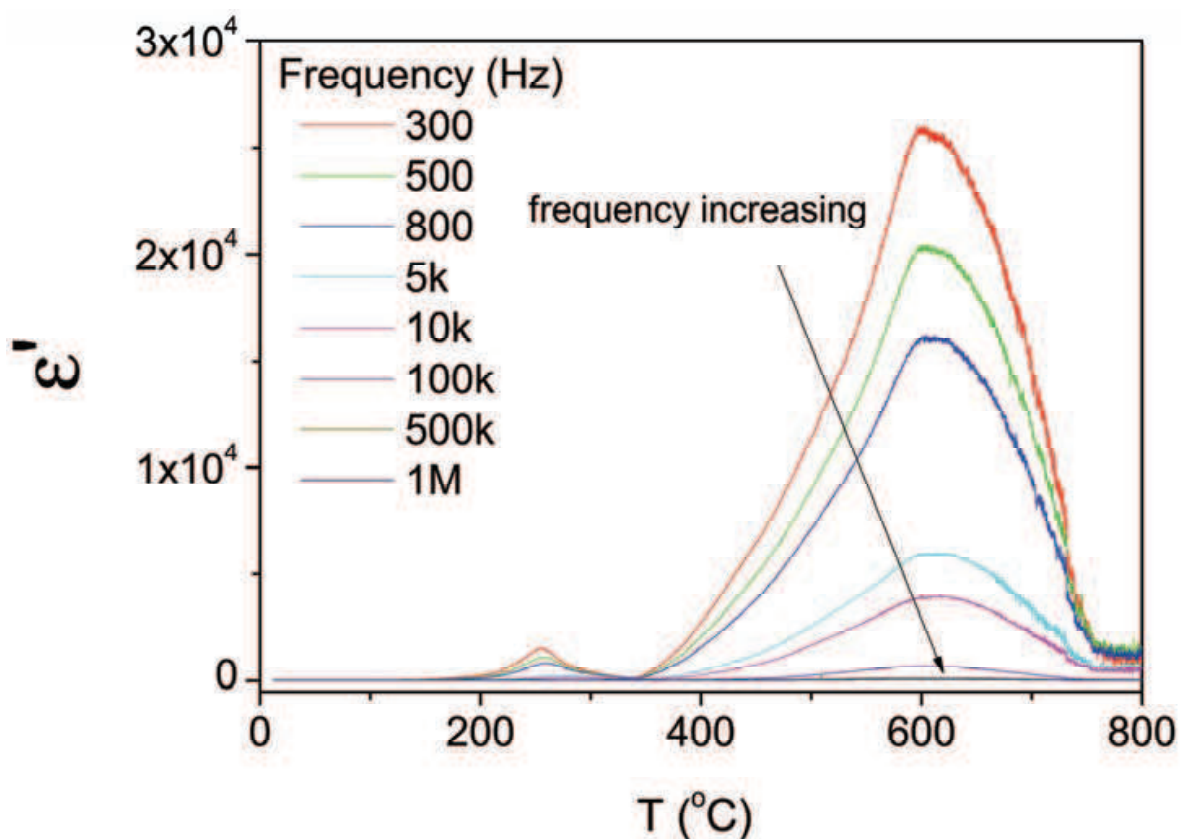


Fig. 1. Temperature dependence of dielectric constant at various frequencies for an as-prepared CTO ceramic sample. By CC Wang et al.

These behaviors are similar to those of relaxors [12]. It seems that the sample might be a relaxor, and therefore, the anomalies are expected to be related to ferroelectric phase transitions. To check out this possibility, we conducted high-temperature XRD measurements. Figure 2 presents the XRD patterns measured at several temperatures. Besides the fact that all the reflections move to lower two theta values with increasing temperature due to thermal expansion, no alien reflections were detected. This indicates that the ilmenite structure maintains to at least the highest measuring temperature of 900 °C. The Jade refinements reveal that the lattice parameter a shown in Fig. 3 exhibits two linear lines with an inflection point of 662 °C, suggesting that CTO undergoes a structural phase transition at the inflecting temperature. This transition temperature is much higher than that of the high-temperature anomaly indicating that the observed anomalies could not be associated with paraelectric-ferroelectric phase transitions, and also suggesting other mechanism underlies the anomalies.

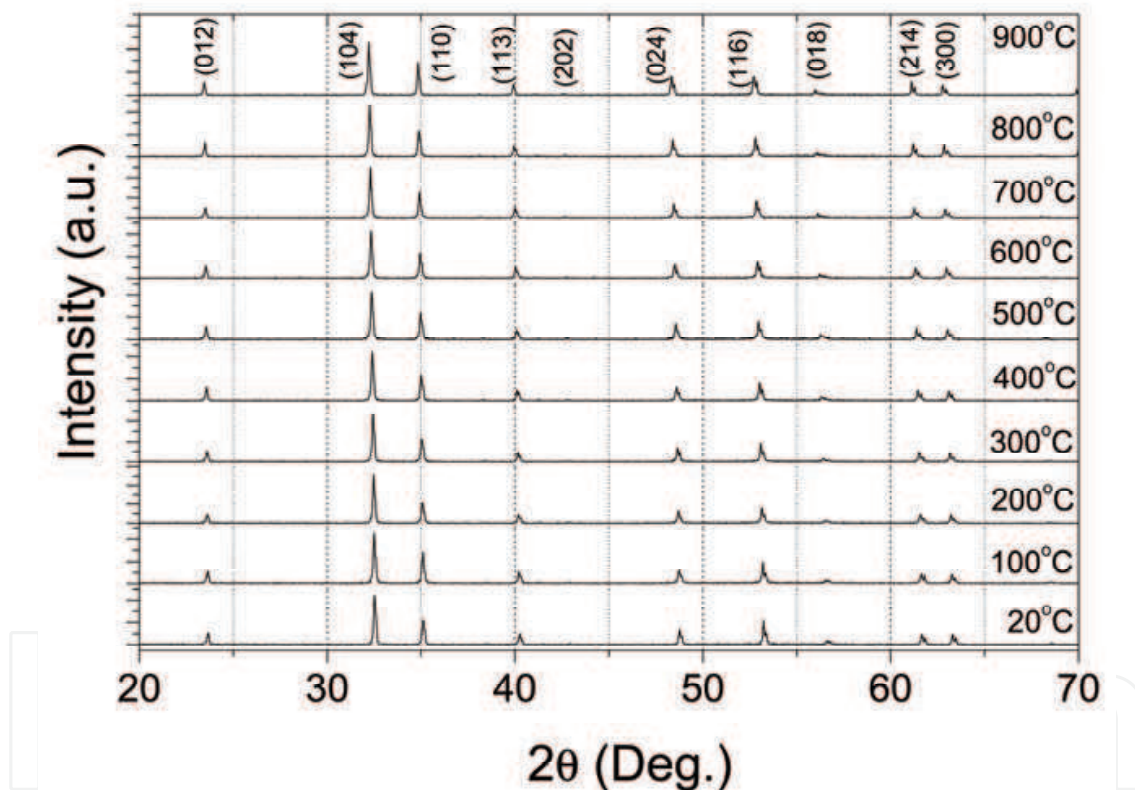


Fig. 2. XRD patterns of CTO sample at several temperatures from room temperature to 900 °C. By CC Wang et al.

To date, several mechanisms unrelated to true relaxor that can produce a relaxor-like anomaly have been proposed. These mechanisms can be classified into three types: (i) the dipole model associated with different mobile defects based on the universal feature that the anomaly is very sensitive to the oxygen vacancy especially for the titanate perovskites [13-15]; (ii) the Maxwell-Wagner model due to electrical inhomogeneity in the tested sample [16-19]; and (iii) the competitive phenomenon between the dielectric relaxation and the electric conduction of the relaxing species [20-22]. Before clarifying which mechanism underlies the

observed anomalies, details about the nature of these anomalies are required. We thus take a careful examination of both ϵ' and loss tangent ($\tan \delta = \epsilon'' / \epsilon'$, where ϵ'' is the imaginary part of the complex permittivity) at 300 Hz in a half-logarithmic representation as displayed in Fig. 4.

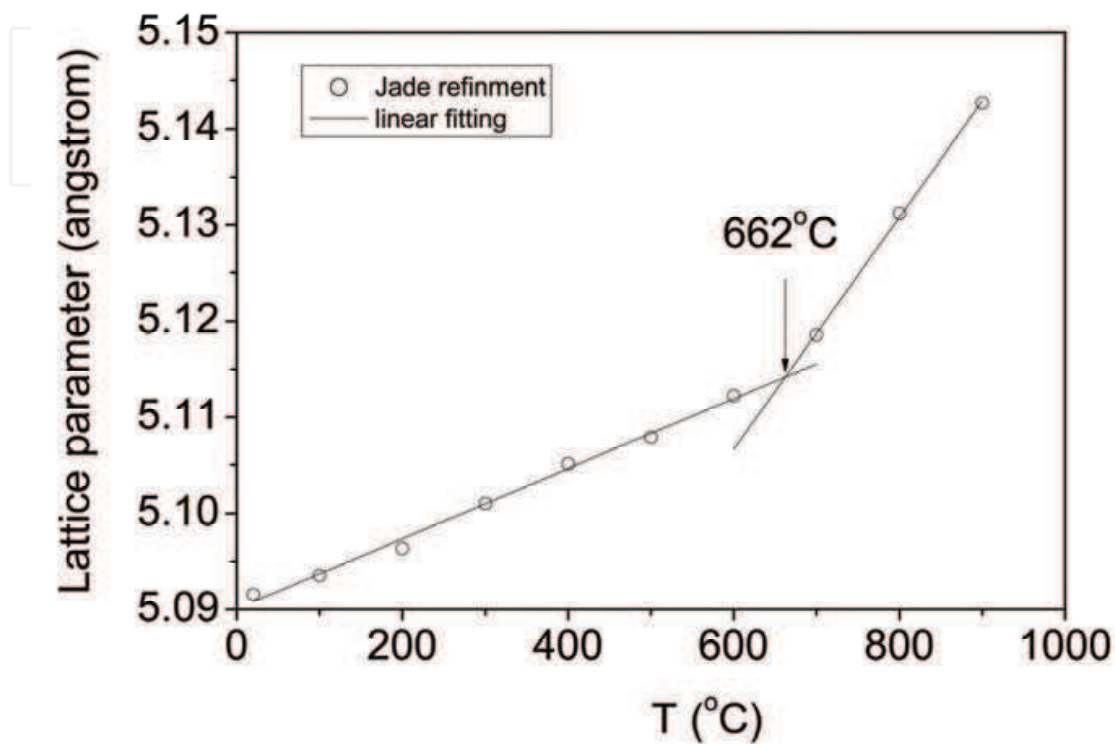


Fig. 3. Lattice parameter as a function of temperature for CTO obtained from the Jade refinements. The inflection point was observed at 662 °C. The straight lines are linear fitting results. By CC Wang et al.

From which some complicated features can be seen: (1) There are two steplike increases in the low-temperature side for each anomaly. The beginnings of the steplike increases were indicated by vertical lines and termed as A, B, C, and D from low- to high-temperature. (2) Corresponding to each beginning of the steplike increase, there exists a peak in loss tangent. Although the peak in $\tan \delta$ for D-steplike increase is invisible because of the increasing background as will be mentioned in the following feature, this peak will be well developed as later discussed by thinning the sample. (3) Corresponding to each anomaly, the $\tan \delta$ increases rapidly with increasing temperature. This feature is much more pronounced in the curve of $\epsilon''(T)$ (not shown here). Since a steplike increase in $\epsilon'(T)$ accompanied by a peak in $\tan \delta(T)$ at the beginning temperature of the increase (or by a peak in $\epsilon''(T)$ at the middle temperature of the increase) is a hallmark for a Debye-type relaxation caused by dipolar or Maxwell-Wagner polarization. This implies that each anomaly contains two Debye-type relaxations. A diffuse dielectric anomaly consisted of two peaks in a thinning sample had been already reported by Stumpe et al in the single crystal of BaTiO₃ [16]. To identify whether the high-temperature anomaly in CTO is composed of two relaxations, we conducted dielectric measurements after two consecutive thinning processes by polishing

the pellet evenly from both sides. After each process, dielectric properties were measured as a function of temperature. The results after each process as well as the result of the as-prepared sample are depicted in Fig.5 for comparison. Compared with the as-prepared sample, it can be clearly seen that the thinned sample exhibits distinct two steplike increases for both anomalies in the curve of $\varepsilon'(T)$ (Fig.5 (a)). Correspondingly, two peaks in loss tangent related to the increases can be well identified (Fig.5 (b)). This result indicates that each anomaly in CTO is truly composed of two relaxations.

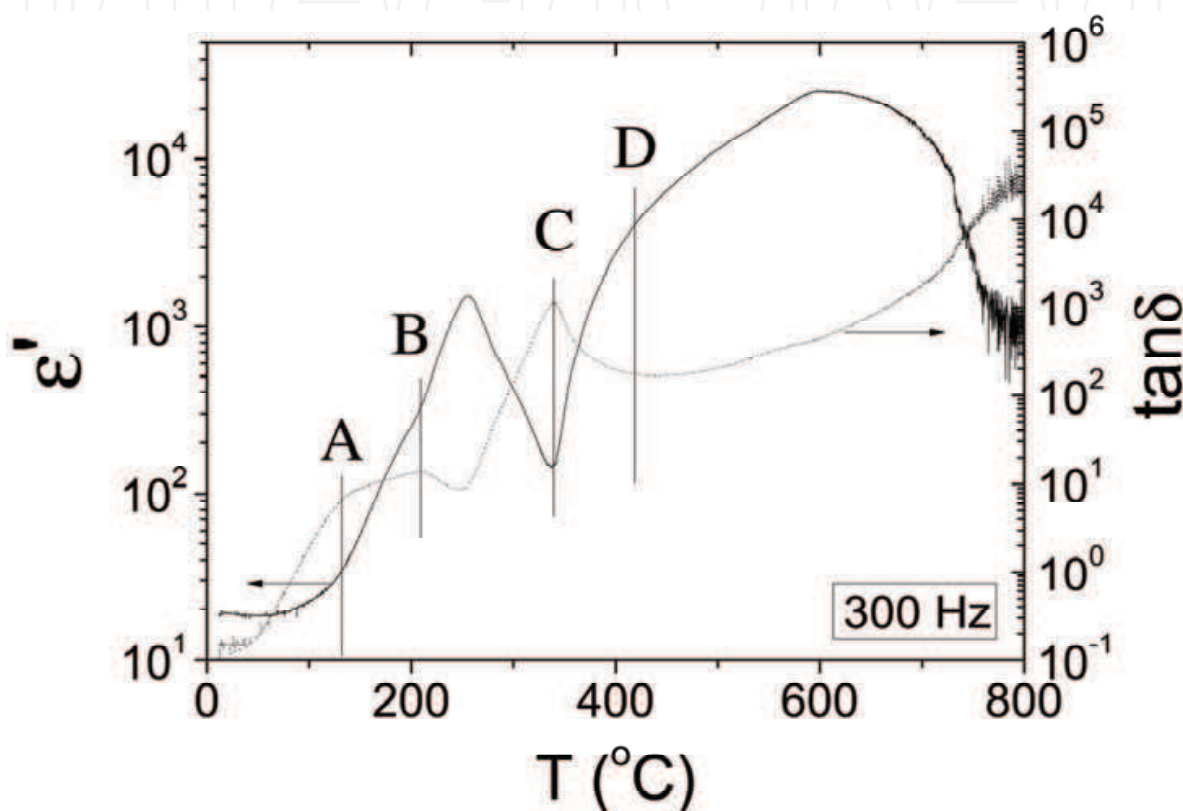


Fig. 4. Temperature dependences of ε' and $\tan\delta$ measured at 300 Hz shown in a half logarithmic scale, which clearly shows some complicated features. By CC Wang et al.

Relaxor-like anomaly was widely reported in various materials [23]. There is a wide consensus that the anomaly appeared in the temperature range of 400 - 900 °C in oxide materials, especially for those containing titanium, is related to oxygen vacancies [13]. This suggests that the high-temperature anomaly in CTO may be related to oxygen vacancy. In order to confirm this inference, the as-prepared sample used in Fig.1 was annealed firstly in O₂ and then in N₂ atmospheres. After each annealing treatment, dielectric properties were measured as a function of temperature. Figure 6 compares the results of $\varepsilon'(T)$ at 300 Hz before (as-prepared) and after O₂- and N₂-annealing treatments. One can clearly see that the O₂-annealing treatment greatly destroys the high-temperature anomaly, but the N₂-annealing treatment enhances this anomaly. But these annealing treatments give rise to opposite effects to the low-temperature anomaly, i.e., oxygen annealing strongly enhances the low-temperature anomaly, and after nitrogen annealing this anomaly even disappears. These results reveal that oxygen vacancies favor for the high-temperature anomaly and

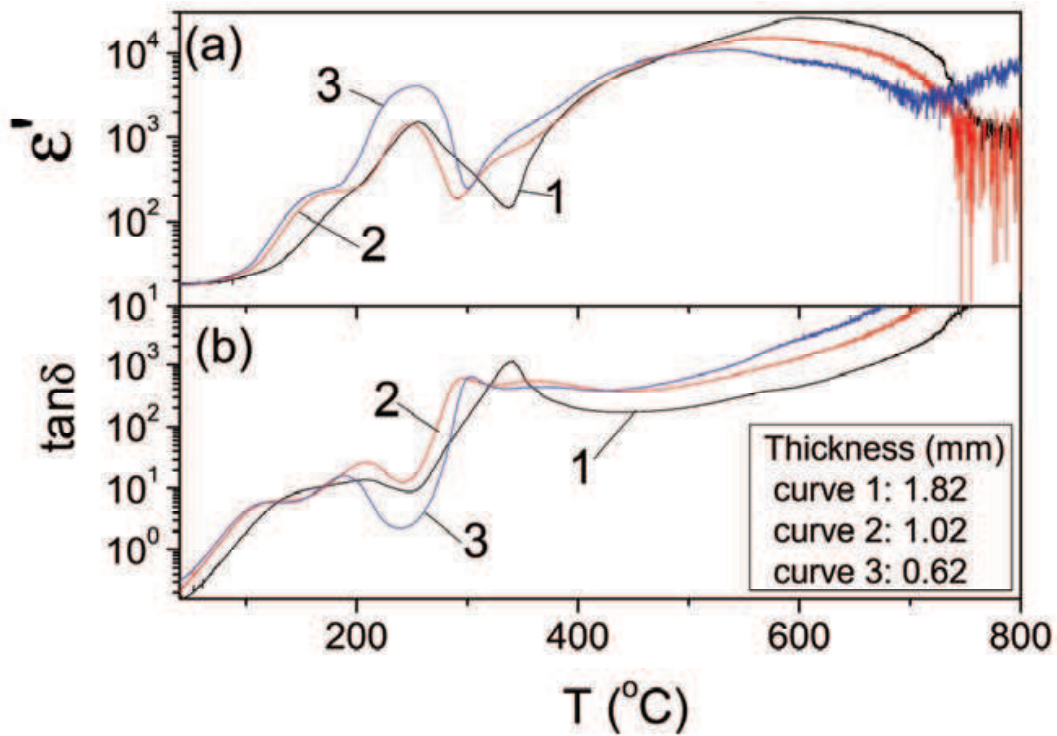


Fig. 5. Temperature dependences of ϵ' (a) and $\tan \delta$ (b) at 300 Hz for the as-prepared (curve 1) and polished (curves 2 and 3) CTO pellet. By CC Wang et al.

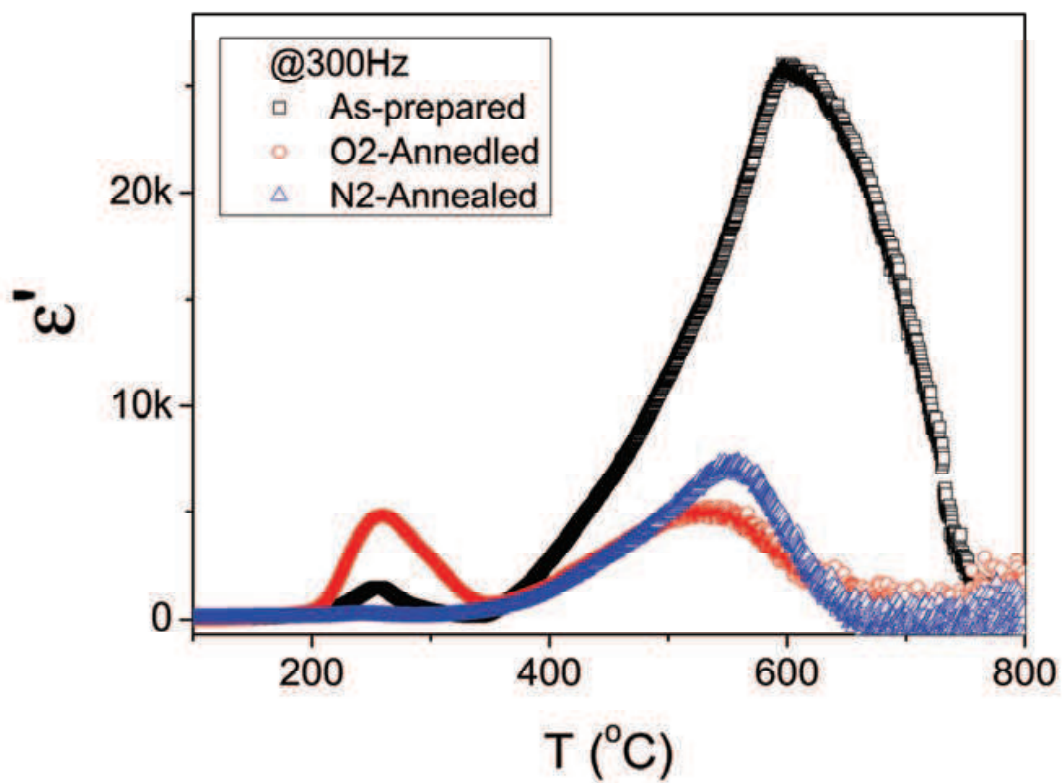


Fig. 6. Comparison of the temperature dependence of ϵ' obtained at 300 Hz for a CTO sample before (as-prepared) and after annealed in high-purity O_2 and N_2 at 800 °C for 2 h. By CC Wang et al.

seriously destroy the low-temperature anomaly. It therefore follows that the oxygen vacancy is truly at the origin of the high-temperature anomaly. It also strongly suggests that the low-temperature anomaly is closely related to positively charged relaxation species, considering the fact that the oxygen vacancies actually act as donors in the sample. Since the cobalt as a volatile element is easy to be lost during the sintering process as reported by many authors [8,24]. The ionization of cobalt vacancies creates holes [8], naturally, the Co vacancies could be suggested as the most probable origin of the low-temperature anomaly. To confirm this point, 5- and 10-wt% Co₃O₄ were added into the resulting CTO powder with the purpose of reducing the Co loss. Details about the preparation of the Co₃O₄-containing samples were given in the experimental procedure. The results of the real and imaginary parts of the dielectric permittivity for the pure and Co₃O₄-containing samples were shown in Fig. 7. From the real part (upper panel), it can be seen that the intensity of the low-temperature anomaly gradually decreases with increasing Co₃O₄ content. This feature can be clearly seen from the imaginary part (lower panel), which also reveals that the rapid increasing background becomes much more remarkable with increasing Co₃O₄ content (please note the logarithmic scale of ϵ''). These results confirm the suggestion that the low-temperature anomaly is associated with Co vacancies.

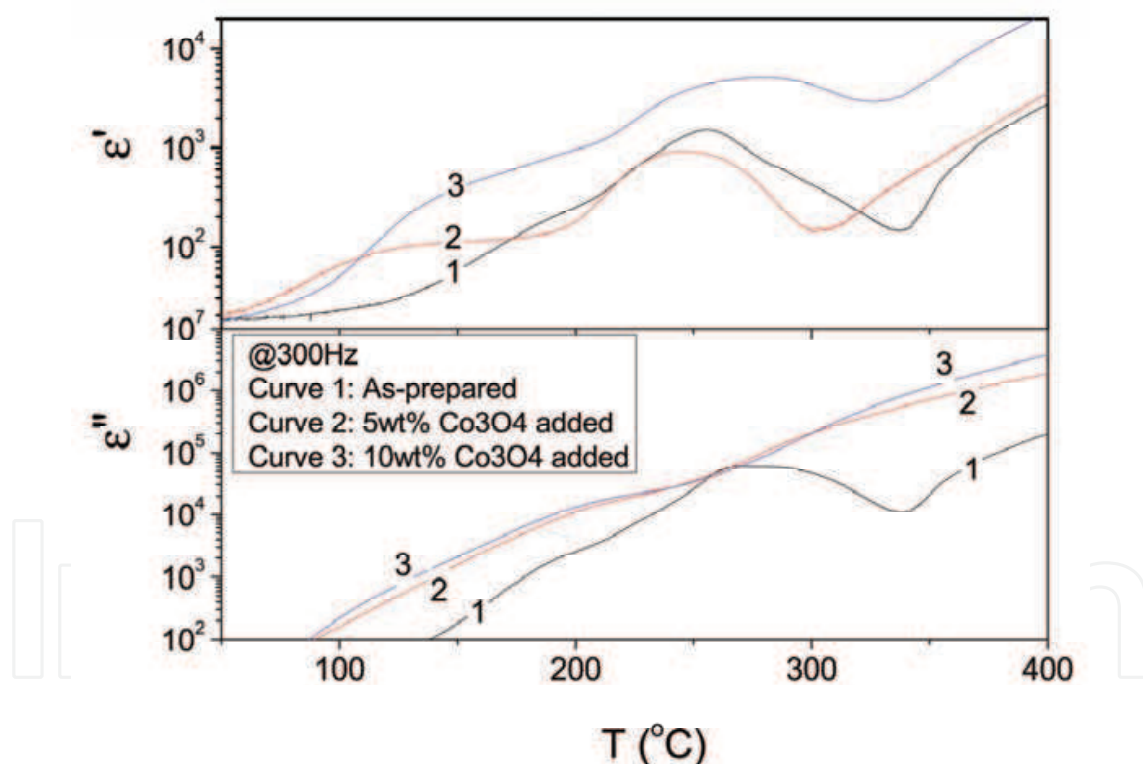


Fig. 7. Temperature dependences of ϵ' (upper panel) and ϵ'' (lower panel) of CTO samples containing various Co₃O₄ contents measured at 300Hz. By CC Wang et al.

It seems clear that the low- and high-temperature anomalies are associated to the cobalt and oxygen vacancies, respectively. However, a pertinent question is, why each of the anomaly contains two relaxation processes? Before answering this question, further information about the nature of the relaxing species is needed. A more sophisticated analysis of the frequency-dependent dielectric behavior can give some insight to this issue. This is done in

Fig.8 showing $\varepsilon''(f)$ for the as-prepared CTO at several selected temperatures. Perfect linear lines were observed in the double-logarithmic representation covering the entire measuring temperature range. This feature indicates that the dielectric behavior follows the universal power law[25], i.e.,

$$\varepsilon'' = B(T)\omega^{s-1} \quad (1)$$

where $B(T)$ and the frequency exponent s (with the value between 0 and 1) are temperature-dependent constants. The values of $s-1$ deduced from the straight lines were plotted in Fig. 9, from which one can see that $s-1$ decreases rapidly with increasing temperature, until at about 250 °C, it registers a peak, then decreases again and reaches a saturation value of -1 at temperatures above 400 °C. Since the value of s actually scales the extent of charger carriers been localized[26], e.g., in the case of $s=0$, Eq. (1) shows the usual reciprocal frequency behavior, and the system is nondispersive transport of free charge carriers process; for $s=1$, Eq. (1) reduces to $\varepsilon'' = \text{constant}$, the system has the feature of nearly constant loss relating to strictly localized carriers [27,28]; while for $0 < s < 1$, the system obeys the universal power law with confined hopping carriers. It, therefore, follows that the relaxing species for the low-temperature anomaly are confined carriers and for the high-temperature anomaly are free ones. The peak in $s-1$ might imply an alteration of the relaxing species changing from acceptor defects (cobalt vacancies) to donor defects (oxygen vacancies).

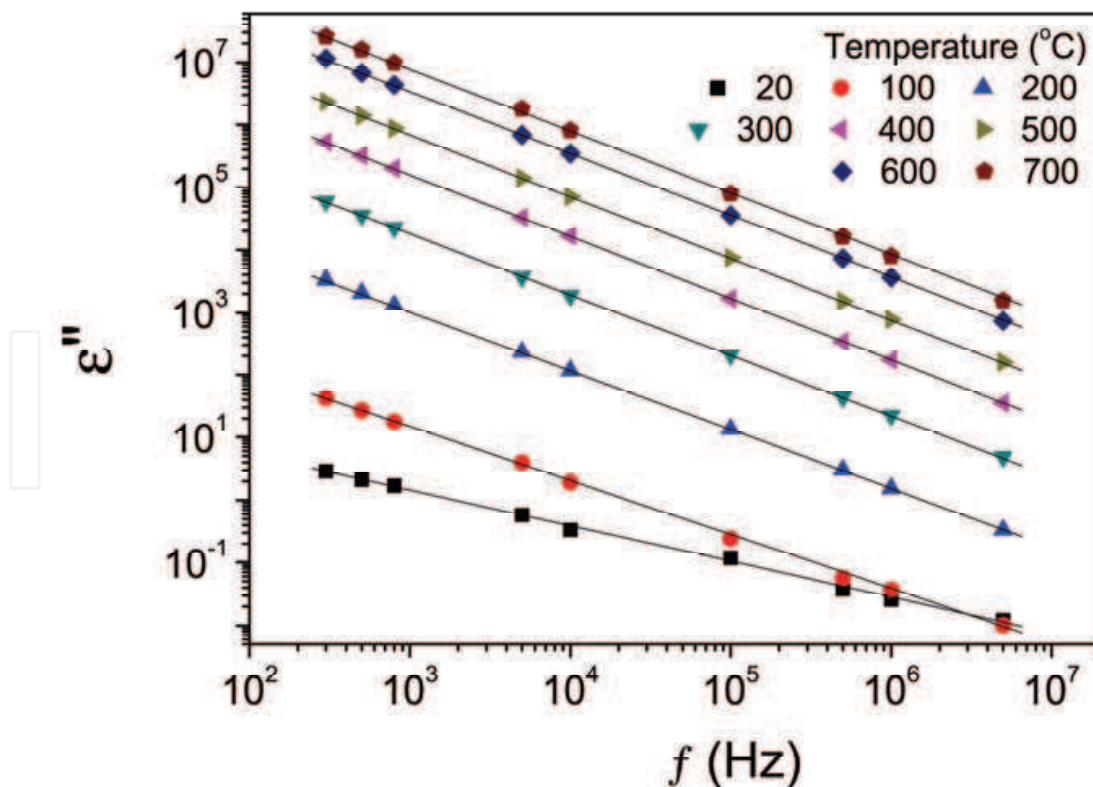


Fig. 8. Frequency dependence of ε'' for the as-prepared CTO sample at various temperatures. The straight lines are linear fitting results. By CC Wang et al.

Based on the nature of the relaxing species, the low- and high-temperature anomalies can be explained reasonably: First of all, the vacancy hopping motions between spatially fluctuating lattice positions not only produce long distance charge transport leading to notable conductivity but also give rise to dipolar effect. The former aspect results in a near-exponential increase in ε'' (or $\tan\delta$) as indicated in Fig. 4; the later makes a significant contribution to dielectric permittivity in the form of dipolar moment-reorientation relaxation under an alternative electric field. Both aspects can be described, as already confirmed, by the universal power law. Furthermore, the long distance transport of vacancies can be blocked by interfaces (e.g., grain boundaries) and sample surfaces, creating space charge there and Maxwell-Wagner relaxation. Therefore, the hopping vacancies can produce both the dipolar and the Maxwell-Wagner relaxations. This is the reason why each anomaly consists of two relaxation processes. Secondly, both relaxations can be described by Debye-like relaxation equations[19,29]:

$$\varepsilon' = \varepsilon_{\infty} + \frac{\varepsilon_s - \varepsilon_{\infty}}{1 + (\omega\tau)^2} \quad (2)$$

$$\varepsilon'' = \frac{(\varepsilon_s - \varepsilon_{\infty})\omega\tau}{1 + (\omega\tau)^2} + \frac{\sigma}{\omega} \quad (3)$$

where ω is the angular frequency, τ is the mean relaxation time, σ is the electrical conductivity of the sample, ε_s and ε_{∞} are the electric permittivity at low- and high-frequency limit, respectively. The relaxation strength, $\Delta\varepsilon$, defined as $\Delta\varepsilon = \varepsilon_s - \varepsilon_{\infty}$, is generally considered as a constant. However, in the case of relaxation processes associated with hopping carriers, the relaxation strength is expressed by[30] $\Delta\varepsilon = N\mu^2 / 3k_B T$, with μ the dipole moment and N the number of the hopping carriers, which varies with temperature following a thermally activated relation:[31]

$$N = N_0 \exp(E / k_B T) \quad (4)$$

where N_0 is the pre-exponential factor, E , the activation energy, and k_B , the Boltzmann constant. One thus has:

$$\Delta\varepsilon = N_0 \exp(E / k_B T) \mu^2 / 3k_B T \quad (5)$$

This equation predicates a nearly exponential decrease in $\varepsilon'(T)$. When the vacancy defect-induced Debye-like relaxation occurs, on one hand, $\varepsilon'(T)$ increases steplike and trends to a saturation value of ε_s ; on the other hand, $\varepsilon''(T)$ decreases rapidly due to the relaxation strength decreases with temperature as predicated by Eq. (5). Therefore, a dielectric peak in $\varepsilon''(T)$, i.e. a dielectric anomaly, should be observed. For the Debye-like relaxation, the steplike increase in $\varepsilon'(T)$, and as a consequence, the anomaly shifts to higher temperatures for higher measuring frequencies, leading to the diffuse nature of the anomaly. So, we can come to the conclusion that the observed anomalies originate from vacancy defect-induced Debye-like relaxations with strongly temperature-dependent relaxation strength. Further evidence supporting this conclusion is the relation between the anomaly intensity and the temperature. Since the Debye-like relaxation occurs around the temperature where $\omega\tau = 1$ is

achieved, the anomaly intensity (Ω) can then be described by the relaxation strength as seen from Eq. (2), viz.

$$\Omega \propto \Delta\varepsilon = N_0 \exp(E / k_B T) \mu^2 / 3k_B T \quad (6)$$

One has:

$$\Omega T \propto N_0 \exp(E / k_B T) \mu^2 / 3k_B \quad (7)$$

Therefore a straight line should be obtained if $\log(\Omega T)$ is plotted as a function of $1/T$. We truly found this linear behavior for the low-temperature anomaly as shown in the inset of Fig. 9. But for the high-temperature anomaly, Eq. (7) is not suitable. This is because that the relaxing species of the low-temperature anomaly are confined cobalt vacancies, whose number will exponentially decrease with increasing temperature as more and more vacancies become free ones. Hence, Eq.(7) works for the confined vacancy defect-induced anomaly. Whereas for the high-temperature anomaly, the number of the relaxing carriers is a constant, because the relaxing species were confirmed to be free ones. In this case, the anomaly intensity should be in proportional to the inverse temperature. This inference was confirmed as seen from the inset of Fig. 9. These results substantially support the point that the observed anomalies are associated with the relaxation processes induced by vacancy defects.

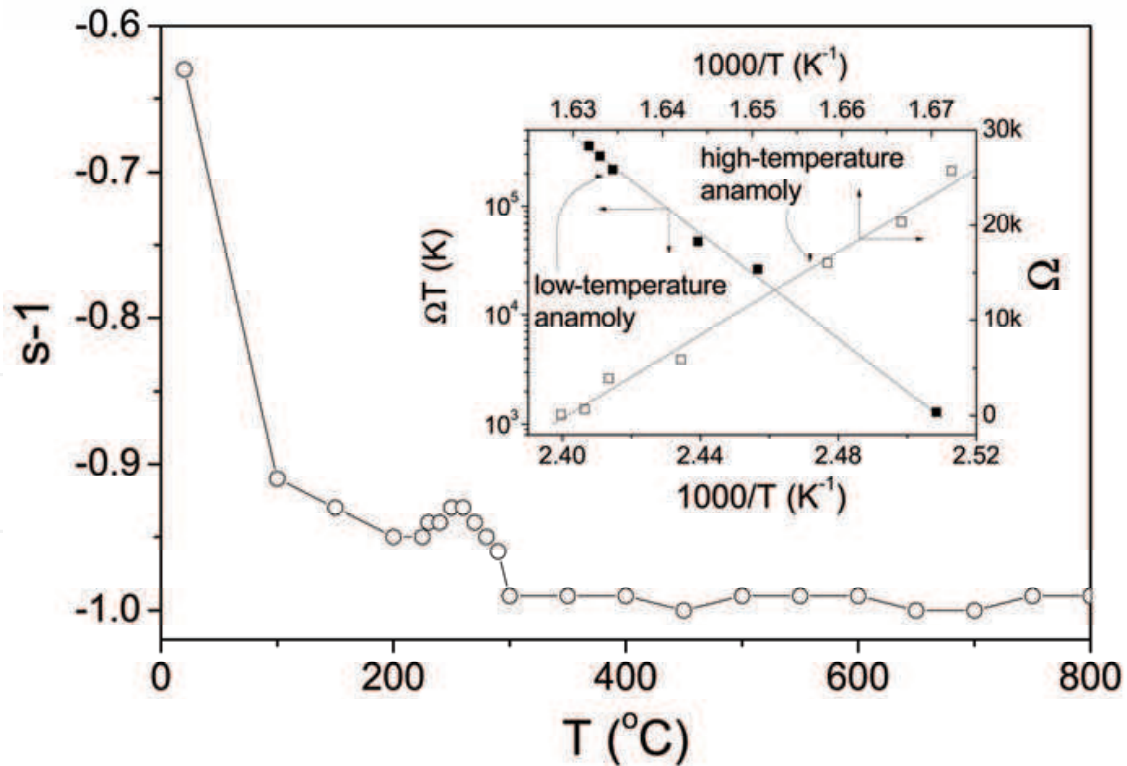


Fig. 9. Temperature dependence of the frequency exponent $s - 1$ deduced from Fig. 8. The inset shows the anomaly intensity as a function of temperature for the low- and high-temperature anomalies. The straight lines in the inset are linear fitting results. By CC Wang et al.

4. Conclusions

In summary, two diffuse dielectric anomalies were observed in CoTiO₃ ceramics. The low-temperature anomaly situated at around 250 °C was found to be related to Co vacancies, while the high-temperature one appeared at about 600 °C was ascribed to O vacancies. The hopping motions of these vacancies firstly create a dipolar relaxation and then a Maxwell-Wagner relaxation as the hopping carriers blocked by the interfaces and surfaces of the samples. Both relaxations obey the Debye-like relaxation equations but with the relaxation strength depending strongly on the temperature. The appearance of the anomalies is a competition process between a $\epsilon'(T)$ increasing process due to the Debye-like relaxation and a $\epsilon'(T)$ decreasing process of the relaxation strength.

5. Acknowledgments

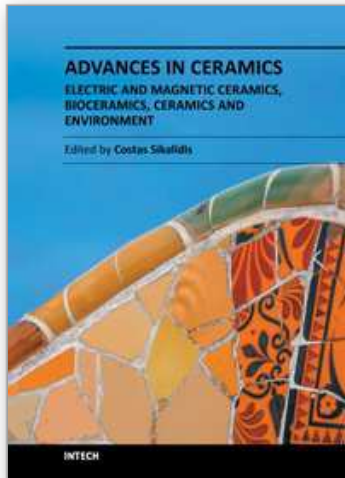
The authors thank financial support from National Natural Science Foundation of China (Grant No. 11074001). This work was supported in part by '211 Project' and Innovative Test Program for Undergraduates of Anhui University.

6. References

- [1] K. H. Buchel and H. H. Moretto, P. Woditsch, *Industrial Inorganic Chemistry*, (second ed., Wiley-VCH, Germany, 2000).
- [2] X. F. Chu, X. Q. Liu, G. Z. Wang, and G. Y. Meng, *Mater. Res. Bull.* 34 (1999) 1789.
- [3] Y. Brik, M. Kacimi, M. ziyad, and F. Bozon-Verduraz, *J. Catal.* 202 (2001) 118.
- [4] T. Kazuyuki, U. Yasuo, T. Shuji, I. Takashi, and U. Akifumi, *J. Am. Chem. Soc.* 106 (1984) 5172.
- [5] N. Dharmaraj, H. C. Park, C. K. Kim, H. Y. Kim, and D. R. Lee, *Mater Chem Phys.* 87 (2004) 5.
- [6] H. T. Kim, S. H. Kim, S. Nahm, and J. D. Dyum, *J. Am. Ceram. Soc.* 82 (1999) 1901.
- [7] P. S. Anjana and M. T. Scbastian, *J. Am. Ceram. Soc.* 89 (2006) 2114.
- [8] C. C. Wang and L. W. Zhang, *J. Phys. D: Appl. Phys.* 40 (2007) 6834.
- [9] T. S. Chao, W. M. Ku, H. C. Lin, D. Landheer, Y. Yang, and Y. Mori, *IEEE Trans. Electr. Dev.* 51 (2004) 2200.
- [10] T. M. Pan, T. F. Lei, and T. S. Chao, *J. Appl. Phys.* 89 (2001) 3447.
- [11] T. M. Pan, T. F. Lei, and T. S. Chao, *Appl. Phys. Lett.* 78 (2001) 1439.
- [12] L. E. Cross, *Ferroelectrics* 76 (1987) 241.
- [13] C. Ang, Z. Yu, L. E. Cross, *Phys. Rev. B* 62 (2000) 228; and references cited therein.
- [14] Z. Yu, C. Ang, P. M. Vilarinho, P. O. Mantas, J. L. Baptista, *J. Appl. Phys.* 83 (1998) 4874.
- [15] A. I. Baranov, *Ferroelectrics* 285 (2003) 225.
- [16] R. Stumpe, D. Wagner, D. Bauerle, *Phys. Stat. Sol. (a)* 75 (1983) 143.
- [17] O. Bidault, P. Goux, M. Kchikech, M. Belkaoui, M. Maglione, *Phys. Rev. B* 49 (1994) 7868.
- [18] D. O'Neill, R. M. Bowman, J. M. Gregg, *Appl. Phys. Lett.* 77 (2000) 1520.
- [19] G. Catalan, D. O'Neill, R.M. Bowman, J. M. Gregg, *Appl. Phys. Lett.* 77 (2000) 3078.
- [20] B. S. Kang, S. K. Choi, C. H. Park, *J. Appl. Phys.* 94 (2003) 1904.

- [21] S. K. Choi, B. S. Kang, Y. W. Cho, and Y. M. Vysochanshii, *J. Electroceramics* 13 (2004) 493.
- [22] B. S. Kang and S. K. Choi, *Solid state Communi.* 121 (2002) 441.
- [23] C. C. Wang and S. X. Dou, *Solid state Communi.* 149 (2009) 2017.
- [24] T. Ogawa, M. Ono, and M. Fujiwara, *Jpn. J. Appl. Phys.* 34 (1995) 5306.
- [25] A. K. Jonscher, *Dielectric Relaxation in Solids* (Chelsea Dielectrics Press, London, 1983).
- [26] C. C. Wang and L. W. Zhang, *New J. Phys.* 9 (2007) 210.
- [27] M. Jain, *Mater. Processes*, 11 (1999) 317.
- [28] A. S. Nowick and B. S. Lim, *Phys. Rev. B* 63 (2001) 184115.
- [29] C. C. Wang, H. B. Lu, K. J. Jin, and G. Z. Yang, *Mod. Phys. Lett. B* 22 (2008) 1297.
- [30] L. L. Hench and J. K. West, *Principles of Electronic Ceramics* (John Wiley & Sons, New York, 1990).
- [31] I. G. Austin and N. F. Mott, *Adv. Phys.* 18 (1969) 41.

IntechOpen



**Advances in Ceramics - Electric and Magnetic Ceramics,
Bioceramics, Ceramics and Environment**

Edited by Prof. Costas Sikalidis

ISBN 978-953-307-350-7

Hard cover, 550 pages

Publisher InTech

Published online 06, September, 2011

Published in print edition September, 2011

The current book consists of twenty-four chapters divided into three sections. Section I includes fourteen chapters in electric and magnetic ceramics which deal with modern specific research on dielectrics and their applications, on nanodielectrics, on piezoceramics, on glass ceramics with para-, anti- or ferro-electric active phases, of varistors ceramics and magnetic ceramics. Section II includes seven chapters in bioceramics which include review information and research results/data on biocompatibility, on medical applications of alumina, zirconia, silicon nitride, ZrO₂, bioglass, apatite-wollastonite glass ceramic and b-tri-calcium phosphate. Section III includes three chapters in applications of ceramics in environmental improvement and protection, in water cleaning, in metal bearing wastes stabilization and in utilization of wastes from ceramic industry in concrete and concrete products.

How to reference

In order to correctly reference this scholarly work, feel free to copy and paste the following:

C. C. Wang, M. N. Zhang, G. J. Wang, and K. B. Xu (2011). Diffuse Dielectric Anomalies in CoTiO₃ at High Temperatures, *Advances in Ceramics - Electric and Magnetic Ceramics, Bioceramics, Ceramics and Environment*, Prof. Costas Sikalidis (Ed.), ISBN: 978-953-307-350-7, InTech, Available from: <http://www.intechopen.com/books/advances-in-ceramics-electric-and-magnetic-ceramics-bioceramics-ceramics-and-environment/diffuse-dielectric-anomalies-in-cotio3-at-high-temperatures>

INTECH
open science | open minds

InTech Europe

University Campus STeP Ri
Slavka Krautzeka 83/A
51000 Rijeka, Croatia
Phone: +385 (51) 770 447
Fax: +385 (51) 686 166
www.intechopen.com

InTech China

Unit 405, Office Block, Hotel Equatorial Shanghai
No.65, Yan An Road (West), Shanghai, 200040, China
中国上海市延安西路65号上海国际贵都大饭店办公楼405单元
Phone: +86-21-62489820
Fax: +86-21-62489821

© 2011 The Author(s). Licensee IntechOpen. This chapter is distributed under the terms of the [Creative Commons Attribution-NonCommercial-ShareAlike-3.0 License](#), which permits use, distribution and reproduction for non-commercial purposes, provided the original is properly cited and derivative works building on this content are distributed under the same license.

IntechOpen

IntechOpen